Modeling Plastic Deformation Effects in Steel on Hysteresis Loops With the Same Maximum Flux Density

Martin J. Sablik, *Senior Member, IEEE*, Taeko Yonamine, and Fernando J.G. Landgraf

***Abstract*—Plastic deformation affects the hysteretic magnetic properties of steels because it changes the dislocation density, which affects domain-wall movement and pinning, and also because it places the specimen under residual strain. An earlier paper proposed a model for computing hysteresis loops on the basis of the effect of grain size d and dislocation density ζ_d. In that paper, hysteresis loops were compared that all had the same maximum flux density $B_{\max}$. The result was that coercivity H_c exhibited a linear relationship with inverse grain size $(1/d)$ and $\zeta_d^{1/2}$. The same was true of hysteresis loss W_H. If one compared hysteresis loops all with the same $H_{\max}$, these linear dependences were only approximately found. Because the relationships are simpler for loops of constant $B_{\max}$, core loss experimenters compare loops that all have the same $B_{\max}$. In this paper, we modify the model to study the effect of plastic tensile deformation on hysteresis loops with the same $B_{\max}$. We found linear relationships between H_c and residual plastic strain ε_r and between W_H and ε_r. With increasing residual tensile strain, H_c increases (whereas with increasing elastic tensile strain, H_c decreases). Also, with increasing residual tensile strain, the slope of the hysteresis loop decreases (whereas with increasing elastic tensile strain, the slope increases). We also consider the effect of compressive plastic deformation.**

***Index Terms*—Hysteresis modeling, magnetic materials, microstructural effects, plastic deformation.**

I. Introduction

IN STEEL, two important microstructural features that affect magnetic hysteresis are: 1) grain size (i.e., average grain diameter d) and 2) dislocation density ζ_d. Since domain walls tend to pin at grain boundaries, the pinning of domain-wall motion increases with increasing total grain boundary length as grain size d decreases. Since coercivity H_c reflects amount and strength of pinning, we expect H_c to increase as d decreases. Similarly, as dislocation density ζ_d increases, dislocations begin to get entangled, forming strong pinning centers for domain walls [1], so impeding domain-wall motion. Thus, as ζ_d increases, so also does H_c. In previous modeling work [2], [3] and in experimental papers [4], [5], it was shown that H_c varies proportionally to $A + B/d$ and $\zeta_d^{1/2}$, where A and B are constants. A similar relationship was also generally found for hysteresis loss W_H [2], [3], [6], [7]. These relationships continue to persist under plastic deformation.

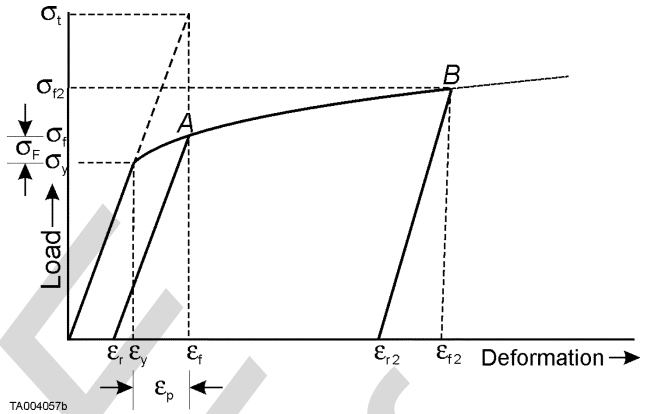

Fig. 1. The left part of the diagram shows a case of small plastic tensile deformation ε_ε after yield. The specimen deforms elastically and linearly up to yield stress σ_y and then deforms plastically to strain ε_f, after which the stress is relaxed to zero and the strain returns elastically to a residual strain ε_r. Note that parameter f, used later, is $f = \sigma_F/(\sigma_t - \sigma_y)$. The right part shows a larger plastic deformation, labeled by subscript 2.

Because many new dislocations are produced under plastic deformation, the dislocation density ζ_d increases and the coercivity H_c and hysteresis loss W_H therefore also increase. The effect of this is to displace the hysteresis loop to higher H and thus to decrease the slope of the hysteresis loop.

A residual deformation ε_r remains after the applied stress σ is removed. We deduce in this paper that with increasing residual tensile strain, H_c increases (whereas with increasing elastic tensile strain, H_c decreases [8]). Also, with increasing residual tensile strain, the slope of the hysteresis loop decreases (whereas with increasing elastic tensile strain, the slope increases [8], [9]). Thus, the residual strain effect on the magnetic properties is just *opposite* to the elastic strain effect in the case of tensile deformation. This effect is seen experimentally as well [1]. Compressive plastic deformation is also discussed.

It should be noted that a hysteresis model has not been fully formulated to date that includes the effect of plastic deformation, so this paper can be viewed as a first attempt. It is expected that further modification of the hysteresis model might be necessary at a later date. Here, we attempt to deal with what we consider to be the chief effects of the plastic deformation.

II. Deformation Model

Fig. 1 shows the deformation model [10] that we will use for tensile deformation. The plot shows applied stress plotted

Manuscript received December 23, 2003; revised May 26, 2004. This work was supported in part by the U.S. National Science Foundation under Grant 0306108 and in part by CNPq in Brazil under the Inter-American Materials Cooperative research program.

M. J. Sablik is with Southwest Research Institute, San Antonio, TX 78228-0510 USA (e-mail: msablik@swri.org).

T. Yonamine and F. J. G. Landgraf are with the Metallurgical Laboratory, Institute for Technological Research (IPT), CEP5508-901 Sao Paulo, Brazil (e-mail: yonamine@ipt.br; landgraf@ipt.br).

Digital Object Identifier 10.1109/TMAG.2004.832763

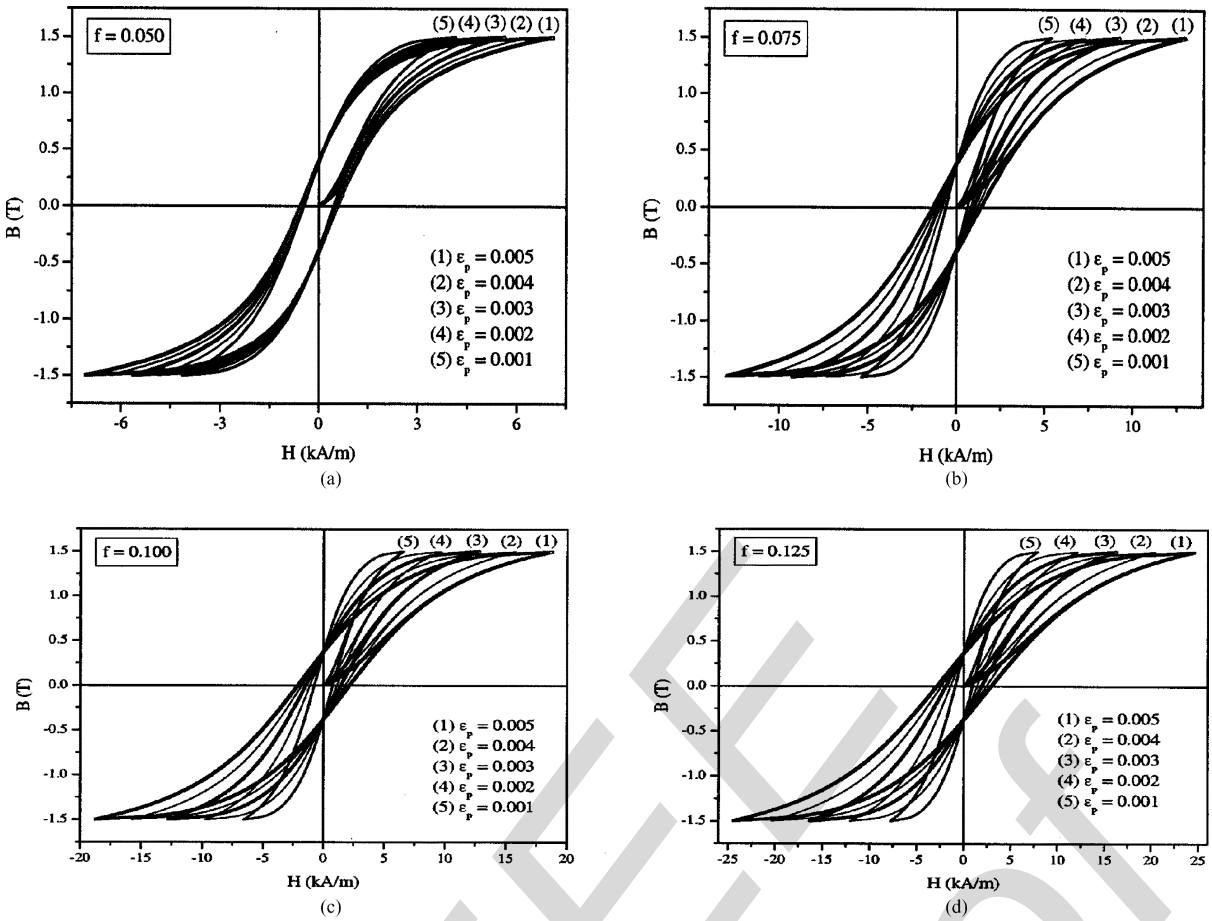

Fig. 2. Hysteresis loops for different strain-hardening stress fractions f. For each f, there are five loops shown for different values of ε_p. All loops are constrained to have the same maximum flux density. All are for tensile deformation.

against deformation ($\varepsilon = \Delta L/L_0$). It is seen that, starting from zero applied stress, the deformation is increased linearly as stress is increased. Once the yield stress σ_y is reached and applied stress continues to be increased, the deformation increases nonlinearly from ε_y until some final deformation ε_f is reached. The deformation $\varepsilon_f - \varepsilon_y$ we shall call ε_p, the plastic deformation after yield. At this deformation, the applied stress has reached a value ε_f. The difference, $\sigma_f - \sigma_y$, is known as the strain hardening stress σ_F [11]. (Another name sometimes used is the flow stress, hence subscript F [12].) σ_F is that part of the stress that is producing plastic deformation. Note that the strain hardening stress σ_F is some fraction f of the total stress after yield (namely $\sigma_t - \sigma_y$), if the initial deformation continued on as an elastic deformation. In other words, $f = \sigma_F/(\sigma_t - \sigma_y)$. Note, too, that $\sigma_t - \sigma_y = Y\varepsilon_p$.

A return path appears in Fig. 1, as indicated by the slanted path downward from point A. If, from σ_f, the applied stress is now decreased back to zero, the deformation ε will decrease linearly, but will not come back to zero when the applied stress becomes zero. A residual deformation ε_r will remain in the specimen as a result of the plastic deformation process. The linear decrease in ε on the return is indicative of an elastic process. Note that in Fig. 1, the return path is parallel to the original elastic path when applied stress was increased. This is a good representation of what happens if deformation ε_p is not too large. If the ε_p is made large enough, then Young's modulus Y can be changed by the deformation, and the slope of the return path will change in that case. In our model in Fig. 1, $Y = Y_0$ for the first return path, but Y is different for the second return path after larger deformation. In our case, we shall take the return path as having the same slope as the initial elastic path, in which case it can be seen from the diagram that

$$\varepsilon_p = \varepsilon_r + \frac{\sigma_F}{Y}. \tag{1}$$

The strain hardening stress is directly related to the dislocation density, and we have the relationship [11]

$$\zeta_d = \left(\left[\frac{|\sigma_F|}{(\alpha_K G b)} \right] + \zeta_{do}^{1/2} \right)^2 \tag{2}$$

where ζ_{do} is the initial dislocation density prior to plastic deformation, G is the specimen shear modulus as given by $G = Y/[2(1+\nu)]$, [11] b is the appropriate Burgers vector magnitude for the specimen's dislocations, ν is Poisson's ratio, and α_K is a constant which [11] gives as 0.76. Note that $|\sigma_F|$ cannot be negative, and so the dislocation density is monotonically increasing regardless of whether the plastic deformation is tensile or compressive, as must physically be the case.

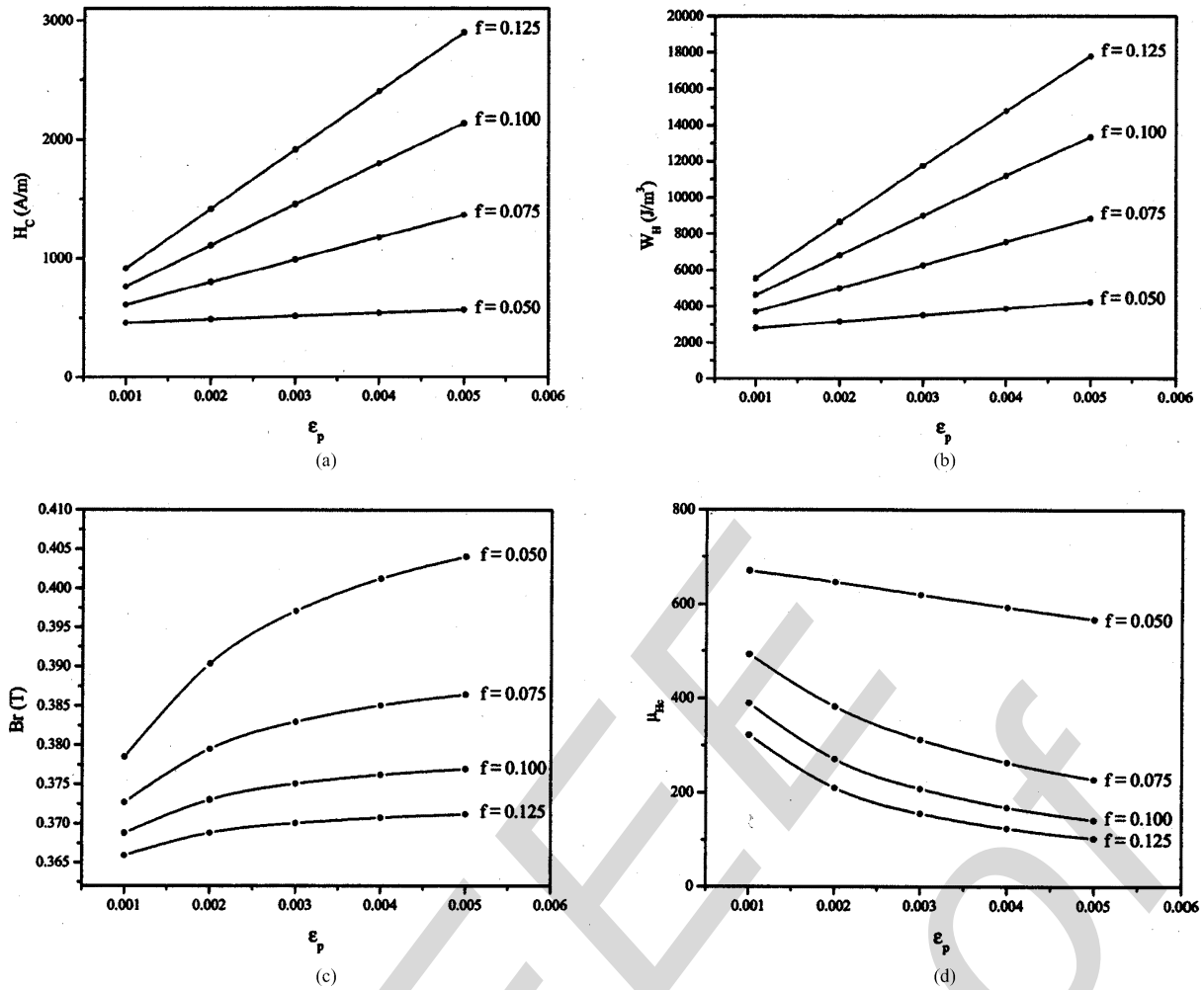

Fig. 3. Four plots, namely (a) H_c versus ε_p, (b) W_H versus ε_p, (c) μ_{Hc} versus ε_p, and (d) B_r versus ε_p, all for tensile ε_p and same maximum flux density as in Fig. 2.

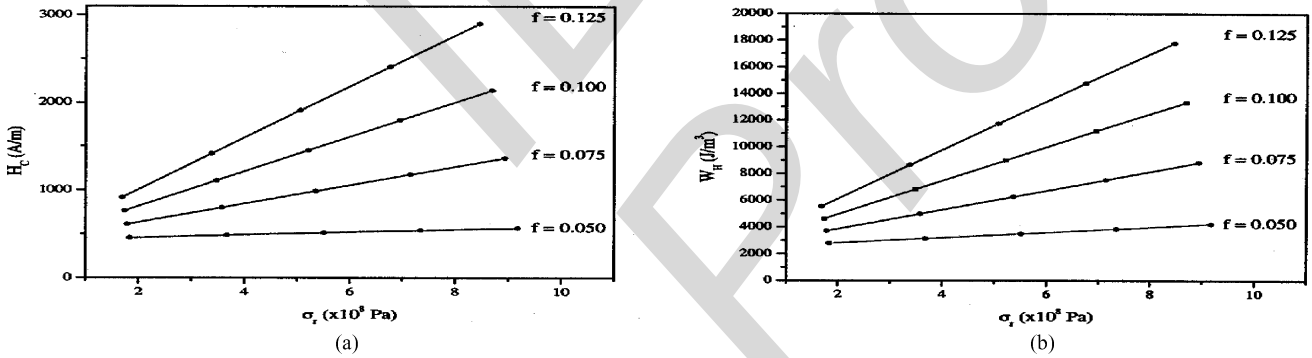

Fig. 4. Plots of (a) H_c versus residual stress σ_r and (b) W_H versus σ_r, evaluated from loops of the same maximum flux density and for tensile deformation.

III. Magnetic Model

We start by referring to the basic hysteresis model of Jiles and Atherton [13], which has been modified to include the effect of stress by Sablik and Jiles [9].

In the Jiles–Atherton model [9], [13], the total magnetization M is the sum of a reversible $(M_{\rm rev})$ and an irreversible $(M_{\rm irr})$ component. These components are given by

$$M_{\rm rev} = c(M_a - M_{\rm irr}) \tag{3}$$

$$M_{\rm irr} = M_a - \frac{k\delta}{\mu_0}\frac{dM_{\rm irr}}{dH_e}. \tag{4}$$

Here, M_a is the anhysteretic magnetization, given as

$$M_a(H_e) = M_s L\left(\frac{H_e}{a}\right) \tag{5}$$

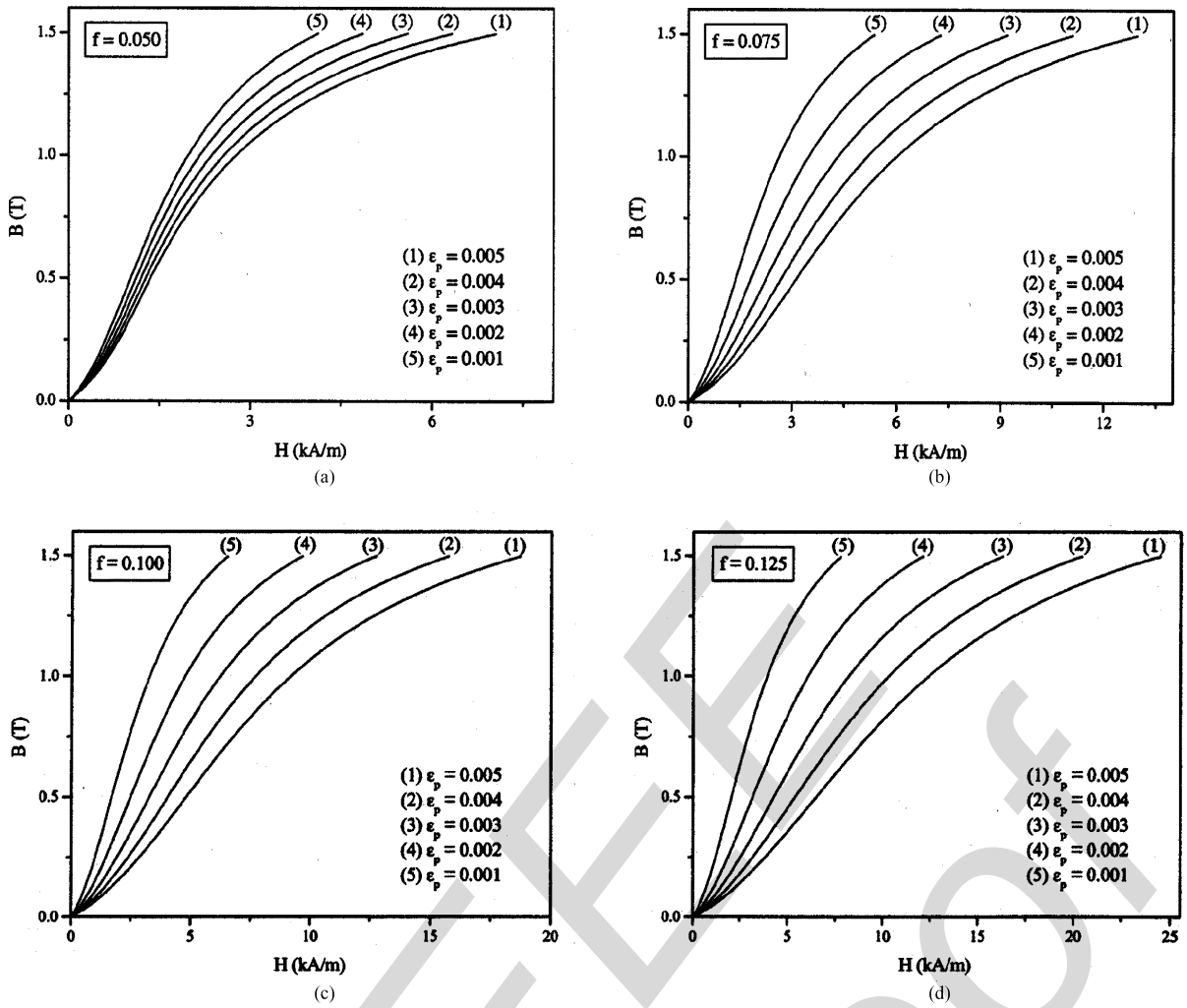

Fig. 5. Various initial magnetization curves (B versus H) up to $B_{\max}$ for specific f and various ε_p and for tensile deformation.

where $L(x) = \coth x - 1/x$ is the so-called Langevin function, and H_e is the effective magnetic field in the material, i.e., [9]

$$H_e = H + \alpha M_a + \left[\frac{3\sigma}{2\mu_0}\right]\left[\frac{d\lambda(M_a)}{dM_a}\right]. \tag{6}$$

The five parameters M_s, c, a, k, and α are all parameters of the material. The parameter δ is $+1$ or -1, depending on whether H is increasing or decreasing. In the last term in (6), σ is the stress acting, μ_0 is the permeability of free space, and $\lambda(M_a)$ is the magnetostriction in the thermodynamic equilibrium state known as the anhysteretic. The last factor in (6) represents the derivative of the anhysteretic magnetostriction with respect to the magnetization in the anhysteretic state. Equation (4) can be reexpressed as a differential equation for $dM_{\rm irr}/dH$ [9], [13]. It is seen that the equations have to be solved self-consistently in numerical fashion.

Since k mathematically controls the amount of hysteresis that is present, it is proportional to the coercivity and hence has the same dependences as the coercivity. Thus, we write [2]

$$k = \left[G_1 + \frac{G_2}{d}\right]\zeta_d^{1/2} k_o. \tag{7}$$

For $d = d^* = 20\ \mu$m and $\zeta_d = \zeta_d^* = 1 \times 10^{12}/\text{m}^2$, we choose G_1 and G_2 so that

$$\left(G_1 + \frac{G_2}{d^*}\right)\left(\zeta_d^*\right)^{1/2} = 1. \tag{8}$$

A choice that satisfies this is $G_2 = 10 \times 10^{-12}$ m^2 and $G_1 = 0.5 \times 10^{-6}$ m. Other choices for G_2 and G_1 also satisfy (8). We find that various choices for G_2 and G_1 correlate with the amount of spread in the hysteresis behavior due to variation of grain size and dislocation density. Note that when d and ζ_d satisfy (8) (i.e., when $d = d^*$ and $\zeta_d = \zeta_d^*$), then $k = k_o$. The 20 μm choice for grain size d^* represents a typical grain size that has been investigated. The choice of $\zeta_d^* = 1 \times 10^{12}/\text{m}^2$ represents a dislocation density quoted by papers on plastic deformation as a typical value for dislocation density in undeformed steel [14], [15] Other papers [2], [16] have quoted values of the order $10^{10}/\text{m}^2$, and such values were used in [2] and [17]. Because the range of ζ_d used here in the absence of plastic deformation is now of order $10^{12}/\text{m}^2$, the values of G_1 and G_2 are altered to accommodate this range.

Scaling constant a is proportional to domain density in the demagnetized state [9], which is determined by pinning site density, which is in turn proportional [13] to pinning constant k.

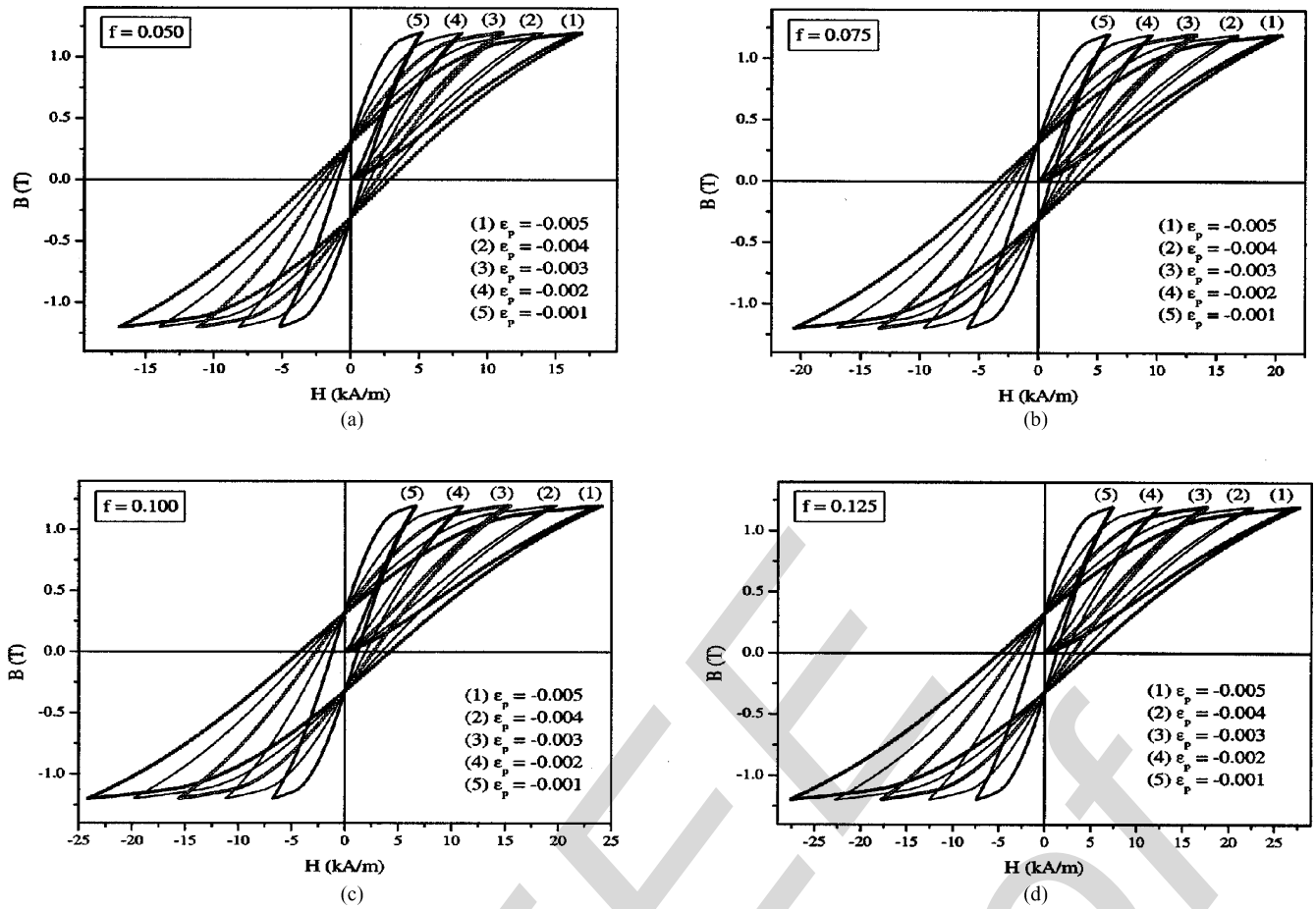

Fig. 6. Hysteresis loops for specimens, which have undergone compressive plastic deformation, for cases of different f and different ε_p.

Thus, a has the same dependence on d and ζ_d that k has, and hence

$$a = \left\{ \left[G_3 + \frac{G_4}{d} \right] \zeta_d^{1/2} \right\} a_o. \tag{9}$$

We have actually showed mathematically [3] in an isotropic nontextured material that a is directly proportional to H_c and hence k. Thus, if we define G_3 and G_4 in the same way as G_1 and G_2, using (9) for $d = d^*$ and $\zeta_d = \zeta_d^*$, then we can set $G_3 = G_1$ and $G_4 = G_2$ and determine a.

Under plastic deformation, we use (2) to compute the dislocation density ζ_d from which the constants a and k are then computed. In the relaxed state after deformation, where there is no applied stress, there is still a residual strain ε_r. This means that there is an additional contribution to the magnetostrictive term in (6), which really devolves from the plastically modified magnetostrain energy. We represent this additional contribution by adding a "residual stress" σ_r to the external stress σ in the last term in (6), where $\sigma_r = Y\varepsilon_r$. When the external stress is zero, the residual stress is substituted for the applied stress in (6), and the material in the specimen will be responsive magnetically to this "residual stress." Thus, the two additional contributions owing to plastic deformation are: i) the *modified dislocation density* arising from the strain hardening stress in (2) and ii) the contribution of the *residual stress*.

Our new input parameters are G, α_K, b, f and either ε_p or ε_r. From these and from Young's modulus Y as a constant of the material, all the other elastic parameters discussed in Section II can be computed.

IV. Results for Tensile Deformation

In the following analysis, we have restricted grain size d to 10 μm. For hysteresis loops all of the same $B_{\max}$, the $B_{\max}$ was chosen by first testing to find the loop that reaches $B_{\max}$ at the largest H and then using its $B_{\max}$ to set the $B_{\max}$ for the rest of the loops. By keeping $B_{\max}$ constant for all the hysteresis loops, we end up with loops of widely varying shape and breadth, as we vary ε_p and f. In particular, we set $\varepsilon_p = 0.001, 0.002, 0.003, 0.004$, and 0.005, and we set $f = 0.050.075, 0.1$, and 0.125. The values for f and ε_p were chosen arbitrarily, and in some steels, could be somewhat larger. For a particular hysteresis loop, to ensure it ends at $B_{\max}$, one increments H in smaller and smaller increments as $B_{\max}$ is neared. Here, we have $c = 0.25$, $k_0/\mu_0 = 500$ A/m, $a_0 = 600$ A/m, $\alpha = 8.44 \times 10^{-6}$ where α is related to λ_s via (30) in [9], and $M_s = 1.585 \times 10^6$ A/m. Both Young's modulus Y and Poisson's ratio ν can be computed from elastic constants C_{11} and C_{12}, [8], [9], which are taken as $C_{11} = 2.863 \times 10^{11}$ N/m^2 and $C_{12} = 1.41 \times 10^{11}$ N/m^2. We also have $b = 2.5 \times 10^{-10}$ m. For G_2 and G_1, we have used the values given just below (6). The parameters are chosen for hard magnetic material.

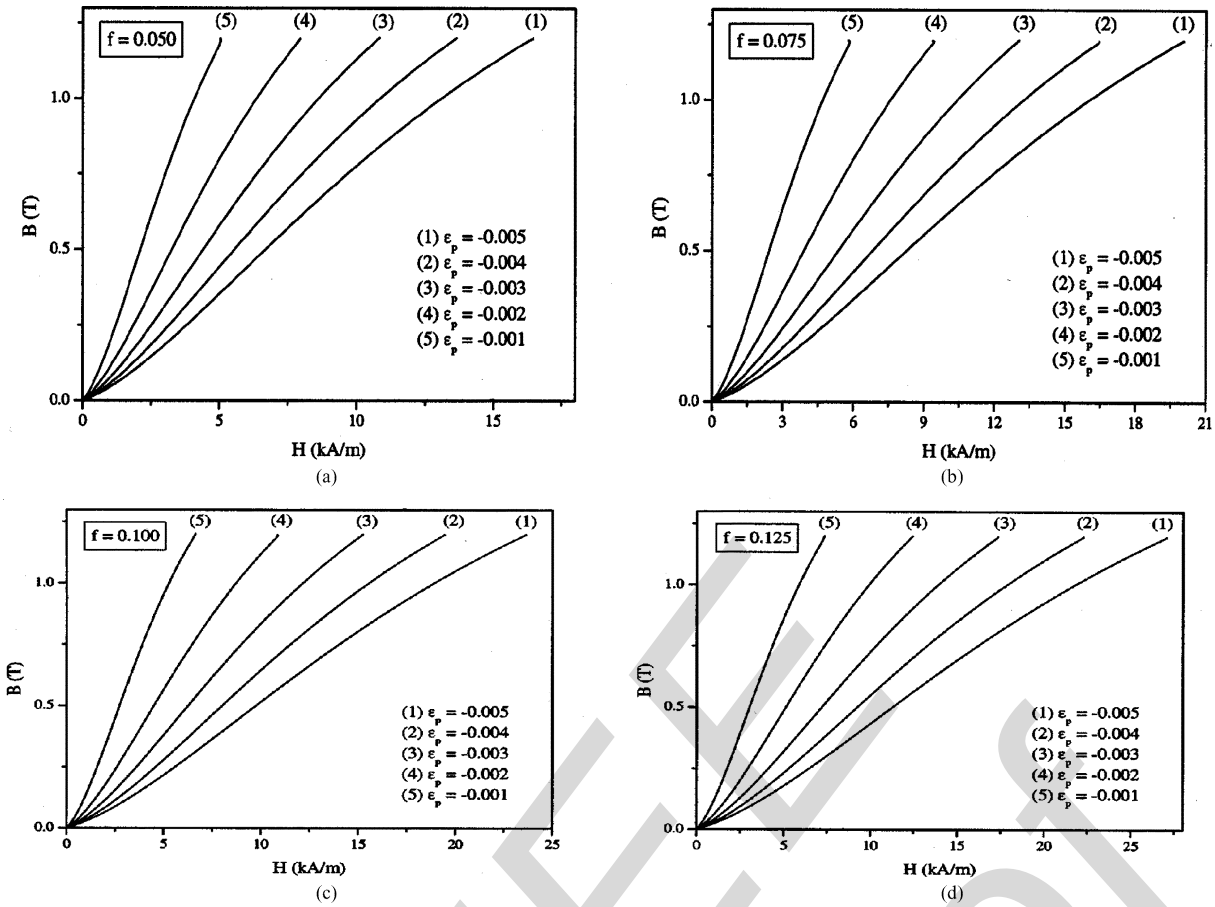

Fig. 7. Various initial magnetization curves (B versus H) up to $B_{\max}$ for specific f and various ε_p, in this case for compressive deformation.

From the various hysteresis loops, we obtain the magnetic properties of coercive field H_c, relative permeability $\mu_{\rm rel} = \mu/\mu_0$ at field $H = H_c$, remanent flux density B_r, and hysteresis loss W_H for each loop. In addition to hysteresis loops, we also obtain the various initial magnetization curves for parameter sets (ε_p, f). The various magnetic properties H_c, B_r, W_H, and $\mu_{\rm rel}$ $(H = H_c)$ have been plotted as functions of ε_p, ε_r, and σ_r.

Fig. 2 shows the hysteresis loops for (a) $f = 0.125$, (b) $f = 0.1$, (c) $f = 0.075$, and (d) $f = 0.05$. For each value of f, five different hysteresis loops are superposed, corresponding to different values of ε_p. It is noted that as ε_p increases, the slopes of the loops decrease but H_c increases. Since greater ε_p implies greater dislocation density ζ_d, one expects the increase in H_c. This qualitatively is what is seen experimentally [1]. One also notes that as f increases, the slopes of the loops decrease and H_c increases. Since larger f implies larger σ_F, again ζ_d and hence H_c increases.

Fig. 3 shows four plots, namely (a) H_c versus ε_p, (b) W_H versus ε_p, (c) μ_{Hc} versus ε_p, and (d) B_r versus ε_p. The most significant point here is that H_c and W_H are linearly dependent on ε_p. This is because ε_p is linearly dependent on σ_F, which is linearly related to $\zeta_d^{1/2}$, which in turn is proportional to H_c and W_H. Only nonlinear relationships exist between μ_{Hc} and ε_p, and between B_r and ε_p. In the case of B_r versus ε_p, there is actually only a small percentage of change in B_r as ε_p changes. This is really not too surprising, since all the loops have the same $B_{\max}$. In the case of differential permeability μ_{Hc} versus increasing tensile plastic deformation, we find that the differential permeability decreases with increasing deformation, which is also found experimentally [18].

Fig. 4 shows two linear plots, similar to Fig. 3(a) and (b), except that here the abscissa variable is the residual stress σ_r, which is proportional to ε_r, which is linearly dependent on σ_F, which in turn is proportional to H_c and W_H, as shown by the plots. A nonlinear relationship is found between μ_{Hc} and σ_r and between B_r and σ_r, similar to what is seen in Fig. 3(c) and (d). We shall not show these plots in order to conserve some space. Note that for this tension case, H_c increases with residual stress, whereas in the elastic case, [8], [9] H_c decreases with elastic stress. The trends for residual stress and the trends for elastic stress are just opposite.

Fig. 5 shows the various initial magnetization curves for the same $B_{\max}$ for the various ε_p in cases of (a) $f = 0.05$, (b) $f = 0.075$, (c) $f = 0.1$, and (d) $f = 0.125$. Note that as ε_p increases, the slope of the initial magnetization curve is less, just as is the case for the hysteresis loops. With the elastic tensile stress [8], [9], the opposite is again true, and for increasing elastic stress, the slope of the initial magnetization curve increases. We thus see once again that increasing residual stress leads to effects that are opposite to increasing elastic stress.

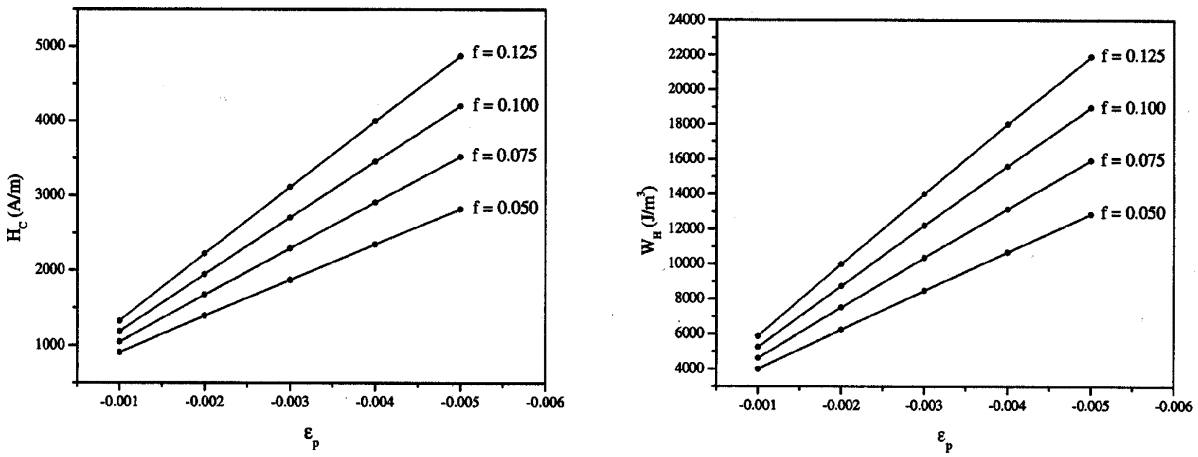

Fig. 8. Plots of H_c and W_H against compressive plastic deformation ε_p, which is negative, for cases of different f and different σ_r.

V. Results for Compressive Deformation

In the case of compressive deformation, the signs for all of the deformations become negative and the signs for all of the stresses become negative. The figure corresponding to Fig. 1 is the same as Fig. 1, except that it exhibits inversion symmetry through origin. In (6), σ is again replaced by σ_r, but this time σ_r is negative. The strain-hardening stress σ_F is also negative, but note that the square root of the dislocation density $\zeta_d^{1/2}$ is related as in (2) to the magnitude of the strain-hardening stress. Hence, from (6), as the strain-hardening stress becomes more negative, the dislocation density becomes more positive and increases. Since that is so, one expects H_c to always increase with increasing plastic deformation magnitude $|\varepsilon_p|$ and increasing residual stress magnitude $|\sigma_r|$. If one had only increasing elastic compressive stress magnitude [8], H_c would also be found to increase. Thus, for compressive stress, increasing residual stress magnitude and increasing elastic stress magnitude produce similar effects on H_c.

This is seen in the hysteresis plots in Fig. 6 for the various cases of ε_p and the different f. There, it is seen that indeed with increasing ε_p magnitude (and hence increasing σ_r magnitude), H_c increases just as in the positive ε_p case. The slope of the hysteresis loop also decreases with increasing ε_p magnitude, just as in the positive ε_p case.

Fig. 7 shows the dependence of the initial magnetization curves for various ε_p and f in the compression case. Note that the slopes of the initial magnetization curves decrease in the compression case for increasing magnitude of ε_p and hence σ_r, just as in the elastic stress case.

Figs. 8 and 9 show that the linear dependences of H_c and W_H on $|\varepsilon_p|$ and $|\sigma_r|$ again occur. It is to be noticed in these figures, however, that intercepts and slopes are not the same as in Figs. 3 and 4. Thus, tensile and compressive plastic deformation are not symmetric in behavior. But even so, these H_c and W_H plots are somewhat similar in appearance.

VI. Conclusion

We have modeled plastic deformation by including that the dislocation density is related to the magnitude of the strain-hardening stress, and by including the magnetoelastic term in the modeling, setting the stress in that term as the residual stress in the case of zero applied stress. In comparing magnetic properties, we compare hysteresis loops all with the same $B_{\max}$. We find that H_c and W_H increase linearly with the deformation magnitude, expressed either as the plastic deformation ε_p after yield or as the residual deformation ε_r which exists after applied stress is brought back to zero. Since ε_r can be reexpressed linearly in terms of the residual stress σ_r, it also follows that H_c and W_H increase linearly with respect to σ_r. This linear increase occurs either with respect to tensile or compressive deformation if expressed with respect to magnitudes, viz. $|\varepsilon_p|$, $|\varepsilon_r|$, or $|\sigma_r|$. The increases for compressive and tensile deformation are not symmetric, in that slopes and intercepts are different with respect to compressive deformation as compared with tensile deformation. If one compares to elastic stress effects, it is found that increasing elastic tensile stress decreases H_c, whereas increasing plastic tensile stress increases H_c. Also, increasing elastic tensile stress increases the slope of the hysteresis loop and the initial magnetization curve, but increasing plastic tensile stress decreases the slope of the hysteresis loop and initial magnetization curve. In other words, the effects of elastic and plastic tensile stress are opposite to each other. On the other hand, elastic and plastic compressive stress magnitudes display the same trends, namely increasing H_c and decreasing the slope of the hysteresis loop and initial magnetization curve. The reason for increasing tensile and compressive plastic stress magnitudes both increasing the H_c is because plastic deformation of either kind causes increased dislocation density, which tends to dominate the magnetic behavior after plastic deformation.

It was mentioned in the introduction that this was a first cut at magnetic hysteresis modeling of the effect of plastic deformation. There does exist a paper which also suggested a magnetic effect of the plastic deformation [19]. This paper noted an effect we did not consider, but did not treat the effects that we have treated. In effect, the paper writes that the domain wall pinning constant should be of the form $k = K_0 - b\lambda_s\sigma$. The paper states that stress should affect pinning, and notes that in the case of steel and elastic stress, this means that coercivity H_c

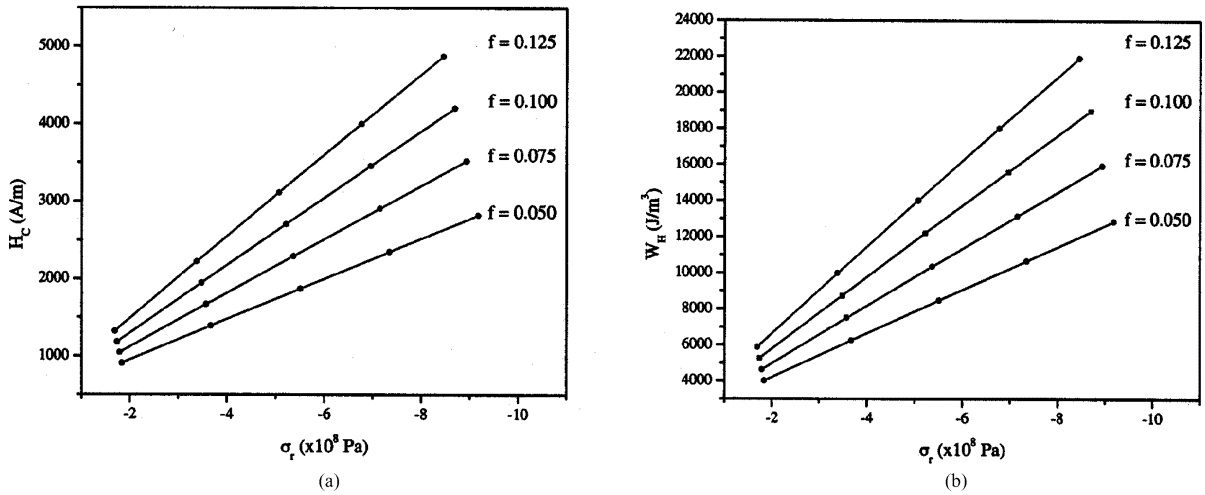

Fig. 9. Plots of H_c and W_H against compressive residual stress σ_r, which is negative, for cases of different f and different σ_r.

will decrease with elastic stress increase, but the first term K_0 depends on dislocation density and will increase under plastic deformation, so producing an increase in H_c. The paper actually dealt with nickel, which has a negative magnetostriction, so that the stress-dependent term in k would add to K_0, so producing an increasing H_c (instead of decreasing) in the elastic region of nickel. While that explained the variation in H_c under tension, it was not a comprehensive model. Nevertheless, it should be interesting to include this precursor model when looking at plastic deformation in a dynamic way and considering cases of nonzero applied stress, which is a project for yet another day.

ACKNOWLEDGMENT

The authors would like to acknowledge the general discussions that they have had with C. J. Gutierrez and H. Kikuchi, which have helped in providing various pieces of important information.

REFERENCES

[1] J. M. Makar and B. K. Tanner, "The in situ measurement of the effect of plastic deformation on the magnetic properties of steel. Part 1—Hysteresis loops and magnetostriction," *J. Magn. Magn. Mater.*, vol. 184, pp. 193–208, 1998.

[2] M. J. Sablik, "Modeling the effect of grain size and dislocation density on hysteretic magnetic properties in steels," *J. Appl. Phys.*, vol. 89, pp. 5610–5613, 2001.

[3] M. J. Sablik and F. J. G. Landgraf, "Modeling microstructural effects on hysteresis loops with the same maximum flux density," *IEEE Trans. Magn.*, vol. 39, pp. 2528–2530, Sept. 2003.

[4] J. F. Bussiere, "On-line measurement of the microstructure and mechanical properties of steel," *Mater. Eval.*, vol. 44, pp. 560–567, 1986.

[5] J. Sternberk, E. Kratochilova, A. Gemperle, V. Faja, and V. Walder, "Dependence of characteristics of hysteresis loops on dislocation density for low-alloy Cr-Mo steel," *Czech. J. Phys. B*, vol. 35, pp. 1259–1267, 1985.

[6] C. Appino, E. Ferrara, F. Fiorillo, I. Suberbielle, J. Degauque, C. Lebourg, and M. Baricco, "Role of Si concentration on the magnetic and mechanical behavior of rapidly solidified Fe-Si laminations," *J. Phys. IV France*, vol. 8, pp. Pr2-531–Pr2-534, 1998.

[7] G. Ban, P. E. Di Nunzio, S. Cicale, and T. Belgrand, "Identification of microstructure effects in magnetic loss behavior of 3.2% SiFe N.O. electrical steels by means of statistical power: Loss model," *IEEE Trans. Magn.*, vol. 34, pp. 1174–1176, July 1998.

[8] M. J. Sablik, S. W. Rubin, L. A. Riley, D. C. Jiles, D. A. Kaminski, and S. B. Biner, "A model for hysteretic magnetic properties under the application of noncoaxial stress and field," *J. Appl. Phys.*, vol. 74, pp. 480–488, 1993.

[9] M. J. Sablik and D. C. Jiles, "Coupled magnetoelastic theory of magnetic and magnetostrictive hysteresis," *IEEE Trans. Magn.*, vol. 29, pp. 2113–2123, July 1993.

[10] G. E. Dieter, *Mechanical Metallurgy*, 3rd ed. New York: McGraw-Hill, 1986, ch. 8, p. 277.

[11] B. Astie, J. Degauque, J. L. Porteseil, and R. Vergne, "Influence of the dislocation structures on the magnetic and magnetomechanical properties of high-purity iron," *IEEE Trans. Magn.*, vol. 17, pp. 2929–2931, Nov. 1981.

[12] H. Kronmuller, "Magnetic techniques for the study of dislocations in ferromagnetic materials," *Int. J. Nondestr. Test.*, vol. 3, pp. 315–359, 1972.

[13] D. C. Jiles and D. L. Atherton, "Theory of ferromagnetic hysteresis," *J. Magn. Magn. Mater.*, vol. 61, pp. 48–61, 1986.

[14] A. S. Keh, "Work hardening and deformation sub-structure in iron single crystals deformed by tension at 298 K," *Phil. Mag.*, vol. 12, pp. 9–30, 1965.

[15] E. Lubitz, "Magnetic studies of the dislocation structure of iron single crystals deformed at 295 K," *J. Appl. Phys.*, vol. 4, pp. 51–61, 1974.

[16] A. H. Qureshi and L. N. Chaudhary, "Influence of plastic deformation on coercive field and initial susceptibility of Fe-3.25% Si alloys," *J. Appl. Phys.*, vol. 41, pp. 1042–1043, 1970.

[17] M. J. Sablik, D. Stegemann, and A. Krys, "Modeling grain size and dislocation density effects on harmonics of the magnetic induction," *J. Appl. Phys.*, vol. 89, pp. 7254–7256, 2001.

[18] J. M. Makar and B. K. Tanner, "The in situ measurement of the effect of plastic deformation on the magnetic properties of steel. Pt. II—Permeability curves," *J. Magn. Magn. Mater.*, vol. 187, pp. 353–365, 1998.

[19] C. C. H. Lo, E. Kinser, and D. C. Jiles, "Modeling the interrelating effects of plastic deformation and stress on magnetic properties of materials," *J. Appl. Phys.*, vol. 93, no. 10, pp. 6626–6628, 2003.